AGU PUBLICATIONS

JGR

Journal of Geophysical Research: Biogeosciences

RESEARCH ARTICLE
10.1002/2016JG003333

Key Points:
- Streambed biofilms play a major role in shaping conservative transport patterns
- Biofilm colonization homogenized transport patterns as they grew
- Biofilm mediated anomalous transport could shape biogeochemical cycles in streams

Correspondence to:
A. F. Aubeneau,
aubeneau@purdue.edu

Citation:
Aubeneau, A. F., B. Hanrahan, D. Bolster, and J. Tank (2016), Biofilm growth in gravel bed streams controls solute residence time distributions, *J. Geophys. Res. Biogeosci.*, *121*, doi:10.1002/2016JG003333.

Received 12 JAN 2016
Accepted 11 JUN 2016
Accepted article online 18 JUN 2016

Biofilm growth in gravel bed streams controls solute residence time distributions

A. F. Aubeneau[1], Brittany Hanrahan[2], Diogo Bolster[1], and Jennifer Tank[2]

[1]Department of Civil and Environmental Engineering, University of Notre Dame, Notre Dame, Indiana, USA, [2]Department of Biological Sciences, University of Notre Dame, Notre Dame, Indiana, USA

Abstract Streambed substrates harbor a rich biome responsible for biogeochemical processing in riverine waters. Beyond their biological role, the presence of benthic and hyporheic biofilms can play an important role in influencing large-scale transport of solutes, even for conservative tracers. As biofilms grow and accumulate biomass, they actively interact with and influence surface and subsurface flow patterns. To explore this effect, we conducted experiments at the Notre Dame Linked Ecosystems Experimental Facility in four outdoor streams, each with different gravel beds. Over the course of 20 weeks we conducted transport experiments in each of these streams and observed different patterns in breakthrough curves as biofilms grew on the substrate. Biofilms played a major role in shaping the observed conservative transport patterns. Overall, while the presence of biofilms led to a decreased exchange rate between the fast (mobile) and slow (immobile) parts of the flow domain, water that was exchanged tended to be stored in the slow regions for longer times once biofilms had established. More specifically, we observed enhanced longitudinal dispersion in breakthrough curves as well as broader residence time distributions when biofilms were present. Biofilm colonization over time homogenized transport patterns across the four streams that were originally very distinct. These results indicate that stream biofilms exert a strong control on conservative solute transport in streams, a role that to date has not received enough attention.

1. Introduction

Streams transport the products of erosion and weathering, as well as anthropogenic materials collected from industrial, agricultural, and urban environments. While waterways are efficient transport networks [*Banavar et al.*, 1999; *Rodriguez-Iturbe and Rinaldo*, 2001], they are also important biogeochemical hotspots [*Peterson et al.*, 2001]. Streams are known to efficiently retain and transform organic and inorganic nutrients [*Odum*, 1956; *Mulholland et al.*, 2008; *Butman and Raymond*, 2011; *Cory et al.*, 2014]. Microbial biofilms colonizing organic and inorganic substrates at the sediment-water interface drive important biogeochemical reactions [*Fischer et al.*, 2005; *Aubeneau et al.*, 2015b]. Additionally, sorption within biofilms and finer sediments can retard and immobilize nutrients and contaminants [*Jarvie et al.*, 2005]. In brief, streams are complex heterogeneous systems characterized by a broad distribution of spatial and temporal transport scales influenced by water column, benthic, and subsurface properties.

While the complexity of transport in streams has been widely recognized in recent years (see the extensive review of *Boano et al.* [2014]), few studies have isolated abiotic from biotic characteristics and processes that ultimately control observed transport patterns. In many instances, studies of conservative transport in streams are interpreted using upscaled anomalous transport models that only implicitly account for known broadly distributed travel times in the waterscape. We define anomalous transport as transport with broad delays and travel times that cannot be adequately described by traditional Fickian advection dispersion models. Anomalous transport models are typically characterized by a certain number of fitting parameters, which empirically capture the broad and distributed range of observed behaviors, but little is known as to how these parameters might correlate with inherent physical and biological characteristics of streams [*Hall et al.*, 2002].

Previous studies have noted complex transport behaviors and patterns in streams and demonstrated the existence of anomalous features using experimental [*Haggerty et al.*, 2002] or numerical approaches [*Cardenas*, 2008; *Deng et al.*, 2004]. In many ways, such studies suggest that anomalous transport in streams is not necessarily "anomalous" but rather ubiquitous; it is the norm rather than the exception. A more limited number

of studies have focused on attributing observed patterns and model parameters to particular processes or features inherent to streams. For example, the presence of alluvial deposits is known to induce broad power law like residence time distributions [*Gooseff et al.*, 2005], while surface processes give rise to more constrained residence time distributions (RTDs) [*Valentine and Wood*, 1979; *Ensign and Doyle*, 2005]. Additionally, *Patil et al.* [2012] demonstrated that hydrologic and geomorphic settings induced and influenced broad RTDs, and more recently, *Aubeneau et al.* [2015a], in a controlled laboratory setting, showed how fractal features in bed morphology produces fractal power law scalings in RTDs. Additionally, *Aubeneau et al.* [2014] showed that the structure and size of bed sediments controlled the characteristics of these broad RTDs and thus the parameters of effective, upscaled models.

In this study, we hypothesized that biofilms can meaningfully impact conservative solute transport. Biofilms form complex structures that directly interact with stream flow [*Battin et al.*, 2003; *Arnon et al.*, 2007; *Nikora*, 2010; *Battin et al.*, 2016]. Just as streams flowing on alluvium exchange water with slow-flowing interstitial water, water flowing in and around benthic biofilms can be much slower than the free surface flow, as demonstrated in several studies [*Mulholland et al.*, 1994; *Bottacin-Busolin et al.*, 2009; *Orr et al.*, 2009; *Larned et al.*, 2011]. This could lead to wide distributions of transport timescale characteristic of anomalous transport. We thus hypothesized that anomalous transport characteristics would change with biofilm colonization over time. More specifically, we predicted that the exponent of the power law residence time distributions in the streams would lessen over time as biofilms grew and created complex networks of fine-scale microstructures that would lead to heavier tails, meaning power law tails with a negative exponent closer to zero. To study the role of biofilms on conservative solute transport, we used four different, well-characterized, experimental streams, each containing a unique substrate configuration at the Notre Dame Linked Experimental Ecosystem Facility (ND-LEEF). Previous research in these streams has demonstrated that all four display anomalous but distinct, transport characteristics [*Aubeneau et al.*, 2014]. In this paper, building on those results, we conducted repeated conservative transport experiments over 20 weeks. We started in early summer with clean, uncolonized stream beds. Biofilms then colonized and accumulated naturally over time until senescence in late autumn. No other characteristics were altered over time, so that flow, temperature, and light availability were all similar across streams throughout the experiments.

2. Methods

2.1. Site Description

We conducted our experiments at ND-LEEF, an outdoor facility located in a Saint Joseph County park in Indiana, USA, containing two constructed experimental watersheds (for details please see *ndleef.nd.edu*). The facility has four experimental streams that are each 60 m long and 0.3 m wide. A constant head reservoir feeds all four streams with low-nutrient groundwater that has stayed for a minimum of 48 h within the reservoir, prior to being delivered by gravity to the experimental streams. In all instances discharge was maintained constant at 1.5 L/s in the four streams. The water depth was 5 cm and velocity 15 cm s^{-1} . The travel time in each stream was thus <10 min. The streams are lined with concrete at the bottom. We added 8 cm of substrate to each stream; one was pea gravel (PG) of characteristic size $D_{50} = 0.5$cm (PG), another was coarse gravel of characteristic size $D_{50} = 5$ cm (COB), in a third stream we alternated 2 m long sections with pea gravel and coarse gravel (ALT), while the fourth stream was filled with a 50:50 mix of pea gravel and coarse gravel (MIX). Because of the different bottom roughness, each stream had slightly different water depth and therefore travel times (see section 3). We include photographs of the four streams in Figure 1 from Week 1 (at construction) and from Week 20 for PG and COB, after colonization with naturally occurring biofilm.

2.2. Dye Injections

We conducted repeated conservative tracer additions using rhodamine WT (RWT) in all four streams; the first addition was considered the "clean" bed case which we conducted 24 h after starting the flow to the streams. We conducted successive releases after 3, 7, 10, 12, and 20 weeks. In all cases, we released a pulse of RWT into the surface water at the top of each reach and recorded its passage at a downstream station, located 48 m from the injection point. We chose this distance to avoid downstream boundary effects as well as to ensure mixing across the flow channel [see *Aubeneau et al.*, 2014, for details]. For all releases, we added 10 mg/L RWT injectate designed to achieve a peak concentration in the breakthrough curves of 100 μg L^{-1}. We used Hydrolab Minisondes equipped with a Turner Designs fluorometer to measure RWT concentrations and the sensor has a sensitivity of 0.01 μg/L with a reliable resolution of concentrations over 4 orders of magnitude.

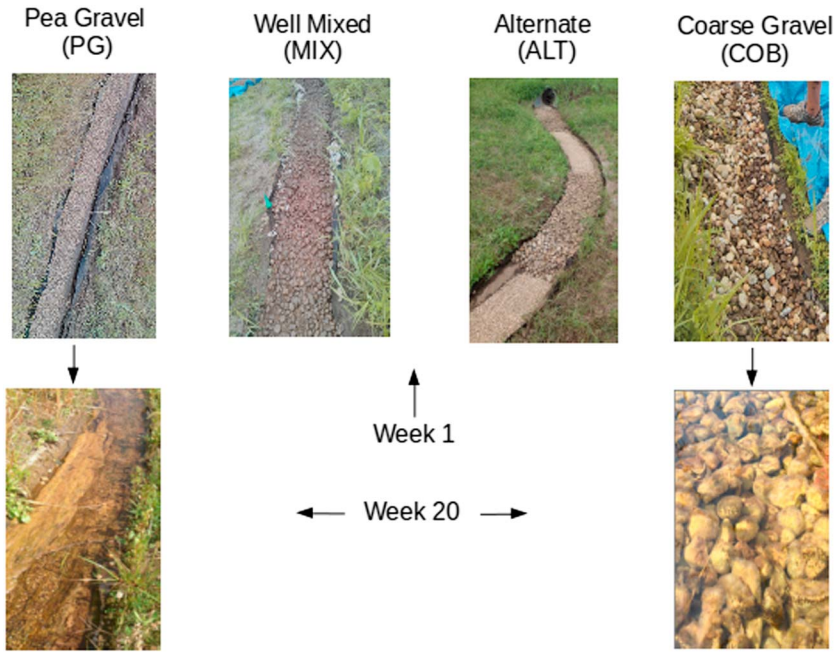

Figure 1. Experimental design, showing the initial and final state. Note the abundant biofilm present at week 20.

2.3. Biofilm Growth

To document biofilm colonization over the duration of the experiment, we measured both benthic organic matter accumulation, expressed as ash-free dry mass (AFDM), and chlorophyll *a* concentration (Chl *a*). We sampled biofilm Chl *a* by collecting benthic samples of a known area from five randomly distributed locations throughout each 50 m stream reach in each of the four streams on each date, by inserting an inverted 160 mL specimen container 2 cm into the substrata following methods in *Hoellein et al.* [2009]. We stored Chl *a* samples on ice, froze them upon return to the lab, and then extracted Chl *a* from each sample and measured it on a fluorometer using standard methods (APHA 1995). We also estimated biofilm AFDM from five randomly distributed locations in each stream by inserting a 314 cm^2 core (5 L bottomless bucket) to the bottom of the concrete-lined channel, then vigorously mixing the substrata, and collecting a subsample of the homogenized slurry using a 160 mL specimen cup. Within 24 h, upon return to the lab, we filtered the subsamples onto preashed and weighed GF/F filters, dried for 48 h at 60°C to measure dry mass, then ashed them at 550°C for 1 h, rewet, and dried for 48 h at 60°C to calculate ash-free dry mass, after loss upon ignition.

2.4. Sorption/Desorption Experiments

In order to test whether RWT sorption played a role in our transport experiments [*Runkel*, 2015], we conducted a series of sorption experiments. We incubated sediments collected from PG and COB in stream water spiked with RWT using eight samples (20–30 mLs each) of sediment collected from the streambed surface, which were colonized with algal biofilms, as well as eight samples collected from below the surface, harboring only heterotrophic biofilms. We placed sediment samples in 150 mL acid-washed glass beakers, covered in aluminum foil to avoid photodegradation, and filled them with 80 mL of stream water, spiking them with RWT to yield concentrations of 0, 0.1, 0.2, 0.4, 0.6, 0.8, and 1 μg/L RWT. We chose to focus on samples ranging from 0–1 μg/L based on a theoretical study by *Aubeneau et al.* [2015b], which suggests these would be the concentrations over which such effects could pose a concern. We placed the beakers on a shaker table for 2 h and transferred 10 mL aliquots into disposable glass test tubes. We also measured duplicate standards and all standards and samples were read on a TD700 fluorometer. We measured one standard curve before the samples, which we measured in random order, interspersed with the duplicate standards to check for instrument drift. We kept all standards and samples in the dark and at room temperature over the 15 min duration to measure all 32 samples and standards. We did not detect any drift or sensitivity issues with the instrument.

2.5. Model

To fit and interpret our breakthrough curve observations, we use an analytical Continuous Time Random Walk (CTRW) model [*Berkowitz et al.*, 2006]. This CTRW framework is a convenient model for transport in surface

flows because it can accommodate any number of RTDs. For narrow distributions, it naturally converges to an ADE as one expects from theory. When one imposes a transient zone with exponentially distributed waiting times, it is analogous to a transient storage model, or equivalently, a single rate mobile-immobile model [*Stonedahl et al.*, 2012]. Additionally, the model can easily represent systems with multiple storage zones, such as a separate hyporheic zone where RTDs are typically broad [*Boano et al.*, 2007; *Aubeneau et al.*, 2015b]. The governing equation for the model is

$$\frac{\partial C(x,t)}{\partial t} = \int_0^t M(t-t') \left[-U \frac{\partial C(x,t')}{\partial x} \mathrm{d}t' + K \frac{\partial^2 C(x,t')}{\partial x^2} \right] \mathrm{d}t', \tag{1}$$

where in Laplace space, M is

$$\tilde{M}(u) = u\bar{t} \frac{\tilde{\psi}(u)}{1-\tilde{\psi}(u)}. \tag{2}$$

C represents the modeled tracer concentration, U and K are the velocity and dispersion in the water column, x is the distance downstream, and t is time. t' is a dummy time variable, $\bar{t}$ is the advective time in the water column, and u is the Laplace variable. M is a memory function where $\tilde{\psi}(u)$ represents the residence time distribution in the whole system, expressed as [*Aubeneau et al.*, 2014]

$$\tilde{\psi}(u) = \frac{1}{1+u+\Lambda-\Lambda\tilde{\varphi}(u)}. \tag{3}$$

In this formulation the model represents a one storage zone model controlled by Λ, the exchange rate between the water column and the storage zone, and $\tilde{\varphi}(u)$, the residence time distribution in the storage zone. In this study, we tested both an exponential distribution, equivalent to a transient storage model, as well as a power law and a truncated power law (TPL) distribution for $\tilde{\varphi}(u)$. In the time domain, the TPL reads [*Aban et al.*, 2006]

$$\varphi(t) = \frac{\alpha t_a^{\alpha} t^{-\alpha-1}}{1-(t_a/T)^{\alpha}} \qquad t_a \le t \le T \tag{4}$$

where t is time, α is the power law exponent, t_a is the lower limit, taken as the advective time of the breakthrough curve, and T is the truncation time. This truncation arises in anomalous transport after all the heterogeneity has been sampled (or equivalently all the timescales have been sampled) and the transport returns to a gaussian behavior [*Aubeneau et al.*, 2014]. To optimize the model prediction and estimate model parameters, we minimized a weighted objective function following *Chakraborty et al.* [2009]. The weights were inversely proportional to the observed values to improve tail fitting. We also used a multistart approach to find global minima.

2.6. Analysis of Variance

The only statistical analysis we performed is an analysis of variance (ANOVA) shown in Figure 4. ANOVAs are a statistical test for heterogeneity of means by analysis of group variances. Here differences were tested between weeks 1, 3, 12, and 20. The null hypothesis is that the mean for each model parameter is invariant in time. A small P value (<0.05) indicates that the null hypothesis is unlikely and that the means are probably different at different times.

3. Results and Discussion

As we predicted, observed transport patterns from our successive RWT releases changed with the biofilm colonization over the 20 week duration of the experiment and breakthrough curves (BTCs) differed over time as shown in PG at weeks 1, 3, 12, and 20 (Figure 2). We also found that the CTRW model fits yielded excellent agreement with the observed field data for RWT concentrations over time. In addition to variation in BTCs over time, BTCs also differed across the four streams on any single collection date (Figure 3); for clarity of presentation, and given the high quality of the fits, we only show the modeled results in this figure. The BTCs from week 1, prior to biofilm colonization in all four streams, clearly show a strong truncation of the late time power law behavior, which varied from stream to stream and was controlled by substrate composition (pea gravel versus coarse gravel) and arrangement (alternating versus well mixed) (see *Aubeneau et al.* [2014] for a detailed discussion). During week 3, we still observe a truncation time in the data, but it was delayed in time

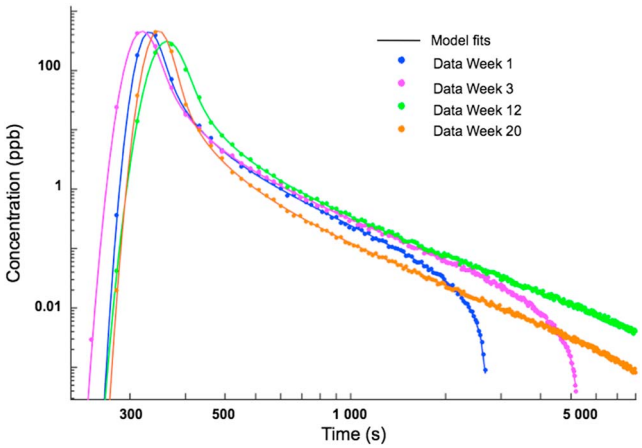

Figure 2. Breakthrough curves in the small gravel stream over time. The dots represent the measured RWT data at weeks 1, 3, 12, and 20 while the light grey lines are the model fits with a truncated power law storage residence time distribution. The power law tail was sharply truncated early in the time series (weeks 1 and 3), while the truncation of the power law tail was no longer visible after biofilm colonization peaked (week 12 and 20).

relative to the week 1 experiments and unlike the week 1 case was now similar in magnitude across all four streams. By week 10, we no longer observed a clear truncation in the BTC data; however, due to the finite extent of our stream beds, one presumably still occurs, but at a time outside our window of observation (3 h or 20 travel times defined as distance divided by mean flow velocity). Qualitatively, all four streams appeared to behave much more similarly after significant biofilm colonization occurred, with power law tails resembling one another, and no longer carrying a clear and marked signature of the specific substrate structure. Additionally, just from visually looking at the data, we observe that the arrival time of the leading edge and peak in RWT concentration changed over the course of the 20 week experiment (Figure 3).

These observations match the quantitative estimates of the CTRW model parameters (Figure 4). The fitted velocities did not statistically change over time and was anecdotally highest during week 3 (Figure 4a, ANOVA $p = 0.53$). This apparent increased velocity of the surface flow could be due to the biofilms smoothing the bottom roughness and decreasing drag. It is notable that the fastest case happened at week 3, during the time when biofilms were present but still actively growing. By the time they were fully developed (weeks 10 and 20), there may have been enough biomass protruding in the flow that the added drag compensated for the presumed lubrication and smoothing of the bottom sediment, resulting in velocities more similar to those observed in the absence of biofilm (week 1).

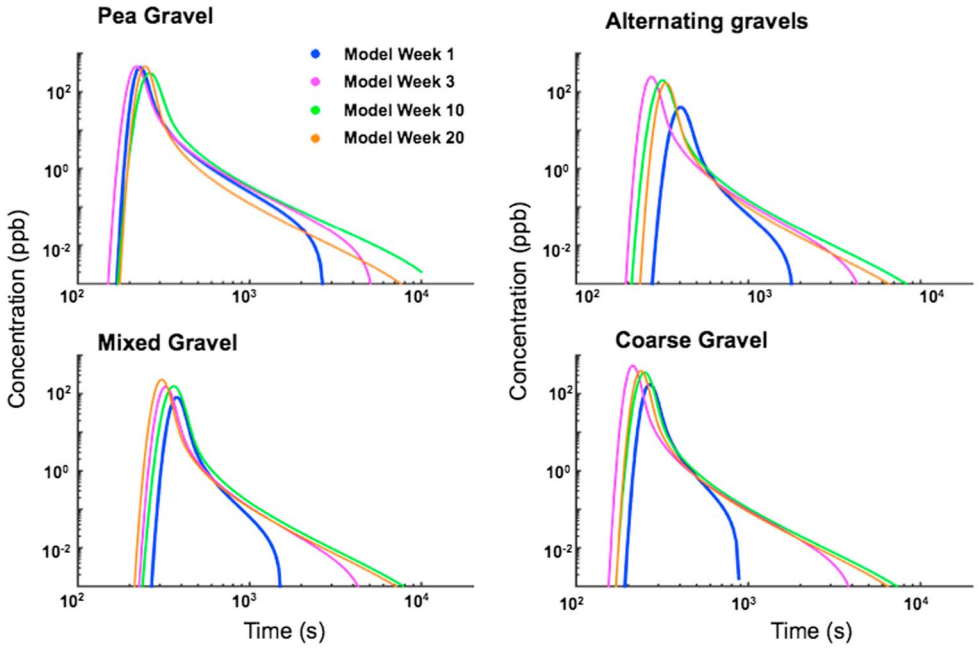

Figure 3. Breakthrough curves in each stream over time. Only the best fit models are shown at weeks 1 (solid line), 3 (dash-doted line), 10 (dashed line), and 20 (dots). The general trend was similar in all four streams, with a sharp truncation early that faded later in the experiments as the biofilms established.

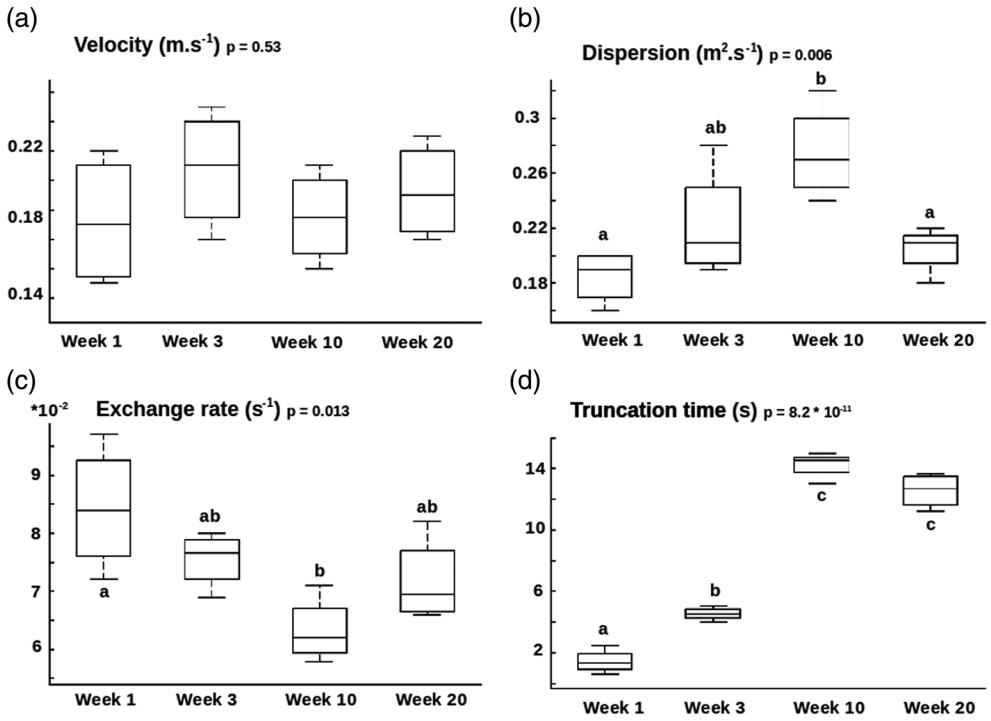

Figure 4. Boxplot of the parameters of a model with a truncated power law hyporheic residence time distribution over time. We present fitted model parameters over time including *p* value resulting from one-way ANOVA with different letters above box plots indicating statistically different means ($n = 4$). For each box plot, the middle line reflects the median, the box is the central 50% of the data, and the bars are the 75% quantile. (a) The velocity did not differ over time, (b) while the dispersion increased significantly before decreasing toward the end of the experiments. (c) The exchange rate between the water column and the storage zone decreased over time, (d) while the truncation time increased.

The dispersion parameter did statically increase over time up to week 10 before decreasing again during week 20 (Figure 4b, ANOVA $p = 0.006$). This suggests that the presence of biofilms increased spreading of the solute in the water column, inducing a broader distribution of velocities and associated travel times. The trends observed in the dispersion coefficient likely reflect features of the biofilms protruding into the open flow. Some water is being trapped and delayed in floating structures and released over time, and this behavior is captured by the dispersion term in the model in the absence of an explicit surface storage zone in the model formulation [*Harvey and Wagner*, 2000]. As the biofilms grew, more and more volume was implicated in those short-term storage processes. By week 20, as the biofilms senesced, some of that biomass had drifted out of our study reaches and the dispersion pattern was more similar to that from earlier experiments.

Long-term retention in slower/immobile parts of the flow domain was also impacted by biofilm colonization. Figure 4c shows that the exchange rate between the flow and the storage zone decreased over time, before bouncing back somewhat at week 20. This suggests that less water may penetrate into the subsurface during weeks 3 and 10 than during week 1 when the biofilms were absent, which likely reflects a progressive clogging of the porous space at the benthic interface that prevented larger exchange rates. By week 20, however, benthic biofilms were senescing and sloughing off, as can be seen in the photographs in Figure 1.

Finally, Figure 4d completes the depiction of the long-term storage behavior. The truncation time of our assessed travel time distribution increased with biofilm growth, and only decreased slightly between weeks 10 and 20. The truncation is no longer clearly visible from the data at these dates and is inferred from the model fit, which means the truncated power law model was extrapolated beyond the measured data. As such, there is less physical constraint on this fitting parameter at the later dates. However, truncation must occur due to the finite extent of our domain but clearly happened later and later as the experiments went on, suggesting that the biofilms did actually modify the physical template producing the observed transport patterns. The additional mass found in the tail for the coarse gravel is about 2 μg after the biofilm colonized or 0.02% of the total mass. Assuming stationarity, 20% of the total mass would be captured by the biofilms after 50 km of

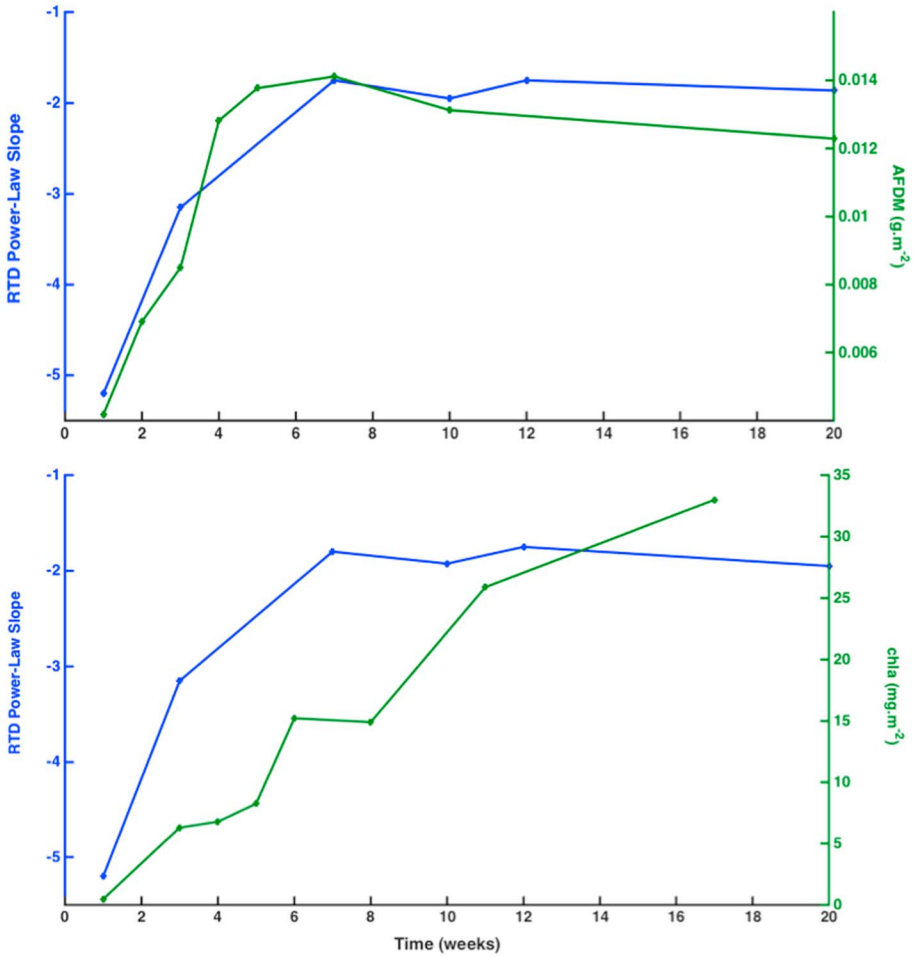

Figure 5. Comparing biofilm growth and power law slopes. This figure compares the decrease in the mean power law slopes for a model with power law distributed storage retention times to the increase in mean biomass, as evaluated by (top) ash-free dry mass and chlorophyll *a* (bottom). There is a clear time correlation between AFDM and power law slopes, suggesting that the growth of the biofilm modified the transport conditions in the streams. Chl *a* on the other hand increased linearly over time.

travel and 100% after 250 km. Even though these numbers are uncertain estimates, they highlight the potentially important role of anomalous transport on overall mass balances and contact time between biofilms and solutes in stream networks.

Biofilms reducing the accessible volume in the porous streambed appear to decrease the amount of exchange between the surface and subsurface; however, the water that actually does make it into this reduced volume pore structure resides there for longer times and takes more time to return to the open water column. Furthermore, the biofilms themselves create new voids and microstructures through which the water also finds its way. These complex growth patterns appear to be directly responsible for water retention over longer periods. This is evidenced by the change during week 20, when more exchange with the slowest compartment was observed and a reduced cutoff time inferred, reflecting the fact that once the biofilms were dying and sloughing off, their presence had less of an influence on large scale transport.

Although to the naked eye the power law slopes observed in Figure 2, particularly during later weeks, seem similar, there are some distinguishing and clear temporal trends that emerge when looking at the data more closely. Figure 5 presents the evolution of the power law slopes for a model with pure power law residence time distribution in the storage zone. This model is distinct from the truncated power law model discussed above as it ignores the existence of a truncation time and therefore emphasizes the power law slope as the main characteristic of the storage behavior. It is essentially a power law fit to the receding part of the breakthrough curves and is a direct measure of the power law observed in the tails of the BTCs. This figure indicates

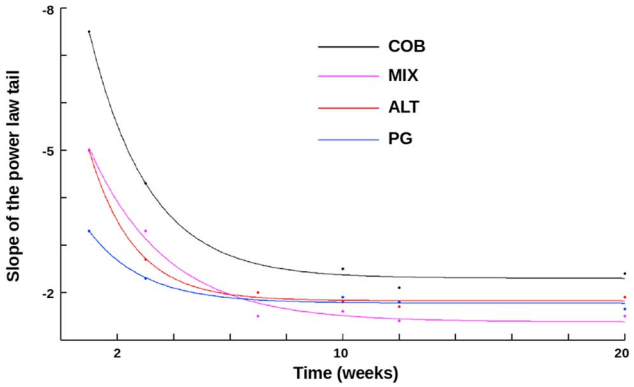

Figure 6. Comparing biofilm growth and power law slopes for each stream. While the general pattern of exponentially decaying slopes (solid lines) was observed in all four treatments, the stream with the coarser gravel (COB) always had a slope steeper than the other streams. The stream with alternating segments was comparable to the stream with the fine gravel asymptotically, and the well-mixed stream had the shallowest slope of all.

that over time, the power law tails become heavier (Figure 5, blue line). This is consistent with our prediction that the biofilm colonization can provide additional complexity and micropores where water would flow more slowly and be retained longer than in bare substrate without biofilm. In addition, we confirm the accumulation of biofilm over time as reflected in the pattern of AFDM over time (Figure 5, top, green line); biofilm AFDM follows a logistic growth with a plateau around week 6. After the biofilm is fully developed, the power law slopes appear to stabilize at values around −2. These two time series are plotted together on the same figure to emphasize their similar trends, suggesting a strong correlation between observed power law retention times and biofilm AFDM. On the other hand chlorophyll *a* concentration increased continuously over time, in an almost linear manner, and did not exhibit the same strong correlation with power law slopes (Figure 5, bottom). This suggests that biofilms occupying the porous space rather than algae at the benthic interface exerted the strongest control on the anomalous behavior. The observed patterns strongly suggest that biological changes in the streams induced the change in the observed transport patterns, supported by the fact that no modifications were made to the streams from week to week, other than allowing the biofilms to accumulate naturally over time. These observations are in line with other studies that have shown that biofilm growth increases micropores' structure and flow complexity [*Battin et al.*, 2016; *Taherzadeh et al.*, 2012].

We found similar support for the correlation when we plotted the evolution of the RTD power law exponent for each stream separately (Figure 6), where the power law slopes decreased exponentially in all four streams, with the solid lines being exponential fits to each stream's own time series (dots). While from the breakthrough curves, particularly at later times, it appears that each of the streams behaved similarly, this figure clearly shows that a unique signature of the substrate template can still be seen throughout the course of the experiments. Thus, while the presence of the biofilms did appear to homogenize behavior across all four streams, as shown by the similar power law slopes toward the end of the experiments, there is still a detectable influence that arises from each unique substrate structure. For example, COB had a power law slope that was consistently higher (i.e., steeper) than all other streams. Coarse substrates are expected to retain fluid for less time than finer ones, which we have previously noted in *Aubeneau et al.* [2014].

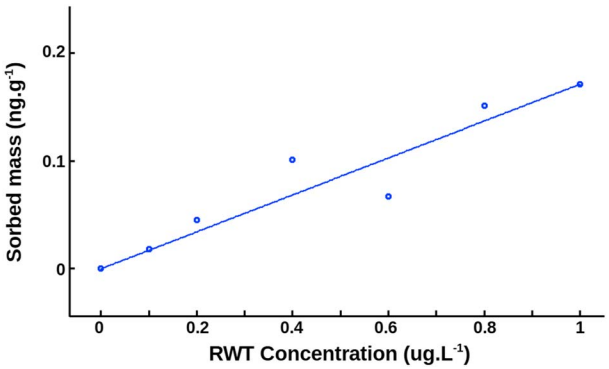

Figure 7. Isotherm showing a very small linear sorption to the sediment at week 13. The line shows a linear fit to the data given by $S = K_d C$, where S is the sorbed mass per g of sediment and C the RWT concentration in $\mu g/L^{-1}$. The resulting partition coefficient $K_d = 0.17 \times 10^{-3}$ L g^{-1}, resulting in minute sorption.

While RWT is often considered a good conservative tracer, it may still sorb to organic matter and therefore be retained preferentially in streams with more biofilms [*Sabatini and Austin*, 1991]. If this sorption is nonlinear, it could influence transport and induce artificial heavy tails in BTCs that could reflect the sorption kinetics rather than physical transport (see our discussion of these issues in *Aubeneau et al.* [2015b]). Even though RWT is known to sorb mostly irreversibly [*Smart and Laidlaw*, 1977], we had good mass recoveries, of at least 90%

and typically 98%. We also conducted batch sorption experiments to measure sorption isotherms and show a typical result in Figure 7. The observed isotherms were linear over the explored RWT range of 0–1 μg/L RWT, and the partition coefficients were always very small. Similar experiments with and without biofilms were repeated for all substrates, and sorption was undetectable on inorganic surfaces (data not shown). We also conducted experiments with sediments taken from the benthic zone, i.e., exposed to sunlight, and from the hyporheic zone, i.e., grown in the dark. The results (not shown) were linear isotherms with comparable small slopes, i.e., the same (small) partition coefficient. We conclude that the measured partition coefficient were so small that little mass should have been influenced by reversible sorption, a statement that agrees with the high mass recovery we measured during our experiments. We also conclude that given the linearity of the isotherms, sorption could not have caused the transport patterns that we presented in this paper.

4. Conclusions

Our experiments demonstrate that biofilm colonization systematically modified RTDs in each of our streams. In particular, we showed that the presence of biofilms increased dispersion and also increased longer-term retention in the experimental streams. Biofilm-induced dispersion has been shown previously, including work that has documented the influence of flow obstructions on transport characteristics [*Valentine and Wood*, 1979; *Ensign and Doyle*, 2005; *Nepf*, 1999]. In addition, enhanced drag and the creation of additional surface storage zones also induces broader BTCs, and *Battin et al.* [2003] showed similar results, where biofilm growth in flumes also increased transient storage over time. Other studies have also reported similar patterns [*Mulholland et al.*, 1994; *Bottacin-Busolin et al.*, 2009; *Orr et al.*, 2009].

To our knowledge, the systematic influence of the presence of biofilms on longer-term retention associated with BTC tails is novel and has not been explored previously. While the role that surface-subsurface exchange plays on anomalous transport has been previously reported [*Haggerty et al.*, 2002; *Wörman et al.*, 2002; *Cardenas*, 2008; *Covino et al.*, 2011], the role played by biofilms has not been explicitly documented, even though biofilms are inherent to streams and colonize all submerged surfaces. Biofilms add a layer of biological microstructures on the physical template [*Lock et al.*, 1984; *Vignaga et al.*, 2013], and the water that travels through these structures experiences velocities that are potentially orders of magnitude slower than those in the free surface open channel flow [*Stoodley et al.*, 1994]. Biofilms thus create conditions for enhanced anomalous transport.

The anomalous transport characteristics were distinct for each stream during week 1 of the experiment, when the streambed substrate had no biofilms (for an extensive discussion on this see *Aubeneau et al.* [2014]). As the biofilms colonized over a period of 20 weeks, differences in BTCs became more subtle (Figures 3 and 4). Our data suggest that one of the primary effects of biofilm colonization is to homogenize conservative transport behavior across the four streams. Despite this apparent visual homogenization, a detailed and quantified look at the data reveals there are still distinguishing features between each of the four streams (Figure 6). Given that biofilms colonize all submerged surfaces within streambeds, their physical effects on solute transport may not always be a simple function of biomass accumulation but rather of the interaction between biotic and abiotic structures.

The streams at ND-LEEF are low gradient and open canopy. We designed the sediment lining to maximize our ability to measure extended residence times and their truncation. Therefore, the stream power to sediment size ratios is unlikely to occur in natural systems. Nonetheless, the principles demonstrated in this paper, in particular the influence of biofilms on long water delays, should be general. Environmental variables such as flow, bed configuration, light availability, and water chemistry (surface water and groundwater) would of course influence the amount of biomass and microhyporheic exchange at a specific site and therefore the local significance of the processes described here.

Given that the fraction of surface water that travels more slowly through subsurface sediments and their associated biofilms may be small, as shown by the small RWT concentrations in the BTC tails, one might ask if these broad travel time distributions are functionally important. For example, if one is concerned about water availability for human use, the first-order control will be the surface channel flow and many of the aforementioned delay processes may not matter. However, if one is interested in water quality, the picture may be quite different, as quality may in many instances be largely controlled by the benthic and hyporheic biogeochemical processes [*Fischer et al.*, 2005; *Larned et al.*, 2004]. As noted above, in the conditions of our experiments, all the surface water could have exchanged with the biofilms within 250 river km. Slow pockets of water are

also known to create the conditions for denitrification [*Briggs et al.*, 2015]. As rivers play a major role in global carbon, nitrogen, and phosphorus budgets [*Raymond and Bauer*, 2001; *Mulholland et al.*, 2008], understanding these slow transport timescales is relevant to a better understanding of global biogeochemical cycles.

Acknowledgments
This work was supported by Notre Dame Environmental Change Initiative and by the National Science Foundation under grants EAR-1344280 and EAR-1113704. We thank the staff at ND-LEEF and St. Patrick's County Park for their logistical support during the experiments. The data may be accessed at aubeneau.com.

References

Aban, I. B., M. M. Meerschaert, and A. K. Panorska (2006), Parameter estimation for the truncated pareto distribution, *J. Am. Stat. Assoc.*, *101*(473), 270–277.
Arnon, S., A. I. Packman, C. G. Peterson, and K. A. Gray (2007), Effects of overlying velocity on periphyton structure and denitrification, *J. Geophys. Res.*, *112*, G01002, doi:10.1029/2006JG000235.
Aubeneau, A., B. Hanrahan, D. Bolster, and J. L. Tank (2014), Substrate size and heterogeneity control anomalous transport in small streams, *Geophys. Res. Lett.*, *41*, 8335–8341, doi:10.1002/2014GL061838.
Aubeneau, A., R. Martin, D. Bolster, R. Schumer, D. Jerolmack, and A. Packman (2015a), Fractal patterns in riverbed morphology produce fractal scaling of water storage times, *Geophys. Res. Lett.*, *42*, 5309–5315, doi:10.1002/2015GL064155.
Aubeneau, A. F., J. D. Drummond, R. Schumer, D. Bolster, J. L. Tank, and A. I. Packman (2015b), Effects of benthic and hyporheic reactive transport on breakthrough curves, *Freshwater Sci.*, *34*, 301–315.
Banavar, J. R., A. Maritan, and A. Rinaldo (1999), Size and form in efficient transportation networks, *Nature*, *399*(6732), 130–132.
Battin, T. J., L. A. Kaplan, J. D. Newbold, and C. M. Hansen (2003), Contributions of microbial biofilms to ecosystem processes in stream mesocosms, *Nature*, *426*(6965), 439–442.
Battin, T. J., K. Besemer, M. M. Bengtsson, A. M. Romani, and A. I. Packmann (2016), The ecology and biogeochemistry of stream biofilms, *Nat. Rev. Microbiol.*, *14*(4), 251–263.
Berkowitz, B., A. Cortis, M. Dentz, and H. Scher (2006), Modeling non-Fickian transport in geological formations as a continuous time random walk, *Rev. Geophys.*, *44*, RG2003, doi:10.1029/2005RG000178.
Boano, F., A. Packman, A. Cortis, R. Revelli, and L. Ridolfi (2007), A continuous time random walk approach to the stream transport of solutes, *Water Resour. Res.*, *43*, W10425, doi:10.1029/2007WR006062.
Boano, F., J. Harvey, A. Marion, A. Packman, R. Revelli, L. Ridolfi, and A. Wörman (2014), Hyporheic flow and transport processes: Mechanisms, models, and biogeochemical implications, *Rev. Geophys.*, *52*, 603–679, doi:10.1002/2012RG000417.
Bottacin-Busolin, A., G. Singer, M. Zaramella, T. J. Battin, and A. Marion (2009), Effects of streambed morphology and biofilm growth on the transient storage of solutes, *Environ. Sci. Technol.*, *43*(19), 7337–7342.
Briggs, M. A., F. D. Day-Lewis, J. P. Zarnetske, and J. W. Harvey (2015), A physical explanation for the development of redox microzones in hyporheic flow, *Geophys. Res. Lett.*, *42*, 4402–4410, doi:10.1002/2015GL064200.
Butman, D., and P. A. Raymond (2011), Significant efflux of carbon dioxide from streams and rivers in the united states, *Nat. Geosci.*, *4*(12), 839–842.
Cardenas, M. B. (2008), Surface water-groundwater interface geomorphology leads to scaling of residence times, *Geophys. Res. Lett.*, *35*, L08402, doi:10.1029/2008GL033753.
Chakraborty, P., M. M. Meerschaert, and C. Y. Lim (2009), Parameter estimation for fractional transport: A particle-tracking approach, *Water Resour. Res.*, *45*, W10415, doi:10.1029/2008WR007577.
Cory, R. M., C. P. Ward, B. C. Crump, and G. W. Kling (2014), Sunlight controls water column processing of carbon in arctic fresh waters, *Science*, *345*(6199), 925–928.
Covino, T., B. McGlynn, and J. Mallard (2011), Stream-groundwater exchange and hydrologic turnover at the network scale, *Water Resour. Res.*, *47*, W12521, doi:10.1029/2011WR010942.
Deng, Z.-Q., V. P. Singh, and L. Bengtsson (2004), Numerical solution of fractional advection-dispersion equation, *J. Hydraul. Eng.*, *130*(5), 422–431.
Ensign, S. H., and M. W. Doyle (2005), In-channel transient storage and associated nutrient retention: Evidence from experimental manipulations, *Limnol. Oceanogr.*, *50*(6), 1740–1751.
Fischer, H., F. Kloep, S. Wilzcek, and M. T. Pusch (2005), A river's liver-microbial processes within the hyporheic zone of a large lowland river, *Biogeochemistry*, *76*(2), 349–371.
Gooseff, M., J. LaNier, R. Haggerty, and K. Kokkeler (2005), Determining in-channel (dead zone) transient storage by comparing solute transport in a bedrock channel–alluvial channel sequence, Oregon, *Water Resour. Res.*, *41*, W06014, doi:10.1029/2004WR003513.
Haggerty, R., S. Wondzell, and M. Johnson (2002), Power-law residence time distribution in the hyporheic zone of a 2nd-order mountain stream, *Geophys. Res. Lett.*, *29*(13), 1640, doi:10.1029/2002GL014743.
Hall, R. O., E. S. Bernhardt, and G. E. Likens (2002), Relating nutrient uptake with transient storage in forested mountain streams, *Limnol. Oceanogr.*, *47*(1), 255–265.
Harvey, J., and B. Wagner (2000), *Quantifying Hydrologic Interactions Between Streams and Their Subsurface Hyporheic Zones*, pp. 3–44, Elsevier, San Diego, Calif., doi:10.1016/b978-012389845-6/50002-8.
Hoellein, T. J., J. L. Tank, E. J. Rosi-Marshall, and S. A. Entrekin (2009), Temporal variation in substratum-specific rates of n uptake and metabolism and their contribution at the stream-reach scale, *J. North Am. Benthol. Soc.*, *28*(2), 305–318.
Jarvie, H. P., M. D. Jürgens, R. J. Williams, C. Neal, J. J. Davies, C. Barrett, and J. White (2005), Role of river bed sediments as sources and sinks of phosphorus across two major eutrophic UK river basins: The Hampshire Avon and Herefordshire Wye, *J. Hydrol.*, *304*(1), 51–74.
Larned, S. T., V. I. Nikora, and B. J. Biggs (2004), Mass-transfer-limited nitrogen and phosphorus uptake by stream periphyton: A conceptual model and experimental evidence, *Limnol. Oceanogr.*, *49*(6), 1992–2000.
Larned, S. T., A. I. Packman, D. R. Plew, and K. Vopel (2011), Interactions between the mat-forming alga *Didymosphenia geminata* and its hydrodynamic environment, *Limnol. Oceanogr.*, *1*(1), 4–22.
Lock, M., R. Wallace, J. Costerton, R. Ventullo, and S. Charlton (1984), River epilithon: Toward a structural-functional model, *Oikos*, *42*, 10–22.
Mulholland, P., A. Steinman, E. Marzolf, D. Hart, and D. DeAngelis (1994), Effect of periphyton biomass on hydraulic characteristics and nutrient cycling in streams, *Oecologia*, *98*(1), 40–47.
Mulholland, P. J., et al. (2008), Stream denitrification across biomes and its response to anthropogenic nitrate loading, *Nature*, *452*(7184), 202–205, doi:10.1038/nature06686.
Nepf, H. (1999), Drag, turbulence, and diffusion in flow through emergent vegetation, *Water Resour. Res.*, *35*(2), 479–489.
Nikora, V. (2010), Hydrodynamics of aquatic ecosystems: An interface between ecology, biomechanics and environmental fluid mechanics, *River Res. Appl.*, *26*(4), 367–384.
Odum, H. T. (1956), Primary production in flowing waters, *Limnol. Oceanogr*, *1*(2), 102–117.

Orr, C. H., J. J. Clark, P. R. Wilcock, J. C. Finlay, and M. W. Doyle (2009), Comparison of morphological and biological control of exchange with transient storage zones in a field-scale flume, *J. Geophys. Res.*, *114*, G02019, doi:10.1029/2008JG000825.

Patil, S., T. P. Covino, A. I. Packman, B. L. McGlynn, J. D. Drummond, R. A. Payn, and R. Schumer (2012), Intrastream variability in solute transport: Hydrologic and geomorphic controls on solute retention, *J. Geophys. Res.*, *118*, 413–422, doi:10.1029/2012JF002455.

Peterson, B. J., et al. (2001), Control of nitrogen export from watersheds by headwater streams, *Science*, *292*(5514), 86–90, doi:10.1126/science.1056874.

Raymond, P. A., and J. E. Bauer (2001), Riverine export of aged terrestrial organic matter to the North Atlantic ocean, *Nature*, *409*(6819), 497–500.

Rodriguez-Iturbe, I., and A. Rinaldo (2001), *Fractal River Basins: Chance and Self-Organization*, Cambridge Univ. Press.

Runkel, R. L. (2015), On the use of rhodamine WT for the characterization of stream hydrodynamics and transient storage, *Water Resour. Res.*, *51*, 6125–6142, doi:10.1002/2015WR017201.

Sabatini, D. A., and T. Austin (1991), Characteristics of rhodamine wt and fluorescein as adsorbing ground-water tracers, *Groundwater*, *29*(3), 341–349.

Smart, P., and I. Laidlaw (1977), An evaluation of some fluorescent dyes for water tracing, *Water Resour. Res.*, *13*(1), 15–33.

Stonedahl, S. H., J. W. Harvey, J. Detty, A. Aubeneau, and A. I. Packman (2012), Physical controls and predictability of stream hyporheic flow evaluated with a multiscale model, *Water Resour. Res.*, *48*, W10513, doi:10.1029/2011WR011582.

Stoodley, P., et al. (1994), Liquid flow in biofilm systems, *Appl. Environ. Microbiol.*, *60*(8), 2711–2716.

Taherzadeh, D., C. Picioreanu, and H. Horn (2012), Mass transfer enhancement in moving biofilm structures, *Biophys. J.*, *102*(7), 1483–1492.

Valentine, E. M., and I. R. Wood (1979), Dispersion in rough rectangular channels, *J. Hydraul. Div.*, *105*(12), 1537–1553.

Vignaga, E., D. M. Sloan, X. Luo, H. Haynes, V. R. Phoenix, and W. T. Sloan (2013), Erosion of biofilm-bound fluvial sediments, *Nat. Geosci.*, *6*(9), 770–774.

Wörman, A., A. I. Packman, H. Johansson, and K. Jonsson (2002), Effect of flow-induced exchange in hyporheic zones on longitudinal transport of solutes in streams and rivers, *Water Resour. Res.*, *38*(1), 15, doi:10.1029/2001WR000769.